THE JOURNAL OF BIOLOGICAL CHEMISTRY
Vol. 278, No. 6, Issue of February 7, pp. 3615–3627, 2003

Printed in U.S.A.

Three Highly Conserved Proteins Catalyze the Conversion of UDP-*N*-acetyl-D-glucosamine to Precursors for the Biosynthesis of O Antigen in *Pseudomonas aeruginosa* O11 and Capsule in *Staphylococcus aureus* Type 5

IMPLICATIONS FOR THE UDP-*N*-ACETYL-L-FUCOSAMINE BIOSYNTHETIC PATHWAY*

Received for publication, April 22, 2002, and in revised form, November 27, 2002
Published, JBC Papers in Press, December 2, 2002, DOI 10.1074/jbc.M203867200

Bernd Kneidinger‡, Katie O'Riordan§, Jianjun Li¶, Jean-Robert Brisson¶, Jean C. Lee§, and Joseph S. Lam‡‖

From the ‡Canadian Bacterial Diseases Network, Department of Microbiology, University of Guelph, Guelph, Ontario N1G 2W1, Canada, the §Channing Laboratory, Department of Medicine, Brigham and Women's Hospital and Harvard Medical School, Boston, Massachusetts 02115, and the ¶Institute for Biological Sciences, National Research Council, Ottawa, Ontario K1A 0R6, Canada

***N*-Acetyl-L-fucosamine is a constituent of surface polysaccharide structures of *Pseudomonas aeruginosa* and *Staphylococcus aureus*. The three *P. aeruginosa* enzymes WbjB, WbjC, and WbjD, as well as the *S. aureus* homologs Cap5E, Cap5F, and Cap5G, involved in the biosynthesis of *N*-acetyl-L-fucosamine have been overexpressed and purified to near homogeneity. Capillary electrophoresis (CE), mass spectroscopy (MS), and nuclear magnetic resonance spectroscopy have been used to elucidate the biosynthesis pathway, which proceeds in five reaction steps. WbjB/Cap5E catalyzed 4,6-dehydration of UDP-*N*-acetyl-D-glucosamine and 3- and 5-epimerization to yield a mixture of three keto-deoxy-sugars. The third intermediate compound was subsequently reduced at C-4 to UDP-2-acetamido-2,6-dideoxy-L-talose by WbjC/Cap5F. Incubation of UDP-2-acetamido-2,6-dideoxy-L-talose (UDP-TalNAc) with WbjD/Cap5G resulted in a new peak separable by CE that demonstrated identical mass and fragmentation patterns by CE-MS/MS to UDP-TalNAc. These results are consistent with WbjD/Cap5G-mediated 2-epimerization of UDP-TalNAc to UDP-FucNAc. A nonpolar gene knockout of *wbjB*, the first of the genes associated with this pathway, was constructed in *P. aeruginosa* serotype O11 strain PA103. The corresponding mutant produced rough lipopolysaccharide devoid of B-band O antigen. This lipopolysaccharide deficiency could be complemented with *P. aeruginosa wbjB* or with the *S. aureus* homolog *cap5E*. Insertional inactivation of either the *cap5G* or *cap5F* genes abolished capsule polysaccharide production in the *S. aureus* strain Newman. Providing the appropriate gene *in trans*, thereby complementing these mutants, fully restored the capsular polysaccharide phenotype.**

Surface carbohydrate structures are important virulence factors of Gram-positive and Gram-negative bacteria. The Gram-negative opportunistic pathogen *Pseudomonas aeruginosa* causes fatal lung infections in patients suffering from the inherited disorder cystic fibrosis; it also affects burn victims and immunocompromised individuals undergoing anticancer chemotherapy and those infected with human immunodeficiency virus. This bacterium produces a variety of polysaccharide structures, one of which is lipopolysaccharide (LPS).[1] LPS is composed of three distinct units: (i) lipid A, which noncovalently binds the molecule into the outer membrane, (ii) the core region that links, and (iii) the O antigen, composed of linear repeats of di- to hexasaccharide units, to the lipid A anchor (1). In the case of *P. aeruginosa*, two different O antigens are made, namely A-band and B-band (2). A-band is a homopolymer of D-rhamnose present in most serotypes, whereas B-band is a serospecific heteropolymer consisting of di- to pentasaccharide repeating units. Differences in B-band repeating units are responsible for the classification into 20 International Antigenic Typing System serotypes (3, 4). Mutants devoid of O antigen are 1000-fold less virulent than wild-type bacteria (5).

Staphylococcus aureus is an important bacterial pathogen responsible for a broad spectrum of human and animal diseases including cutaneous as well as wound infections and more life-threatening infections such as endocarditis and bacteremia. Moreover, *S. aureus* produces numerous exotoxins, some of which cause diseases such as toxic shock syndrome and food poisoning (6). The majority of clinical *S. aureus* isolates produce either a type 5 or type 8 capsule (CP), which renders the organisms resistant to phagocytic uptake (7). Moreover, CP production has been shown to enhance virulence in animal models of infection (8). *S. aureus* is highly efficient at acquiring

* This work was supported by Canadian Institute for Health Research Grant MOP-14687 (to J. S. L.), Natural Science and Engineering Research Council Collaborative Health Research Projects Program Grant 251007-02 (to J. S. L.), National Institutes of Health Grant A129040 (to J. C. L.), and Canadian Institute for Health Research Equipment Grant MMA-41558 for the purchase of the capillary electrophoresis instrument (to J. S. L.). The costs of publication of this article were defrayed in part by the payment of page charges. This article must therefore be hereby marked "*advertisement*" in accordance with 18 U.S.C. Section 1734 solely to indicate this fact.

‖ Recipient of Zellers Senior Scientist and Marsha Morton Scholar Awards from the Canadian Cystic Fibrosis Foundation. To whom correspondence should be addressed. Tel.: 519-824-4120, Ext. 53823; Fax: 519-837-1802; E-mail: jlam@uoguelph.ca.

[1] The abbreviations used are: LPS, lipopolysaccharide; CE, capillary electrophoresis; CP, capsular polysaccharide; HMBC, heteronuclear multiple bond correlation; HSQC, heteronuclear single quantum coherence; mAb, monoclonal antibody; MS, mass spectroscopy; NOE, nuclear Overhauser enhancement; NOESY, NOE spectroscopy; SDR, Short Chain Dehydrogenase/Reductase; TOCSY, total correlation spectroscopy; UDP, uridine diphosphate; UDP-L-FucNAc, UDP-2-acetamido-2,6-dideoxy-L-galactose or UDP-*N*-acetyl-L-fucosamine; UDP-D-GlcNAc, UDP-2-acetamido-2-deoxy-D-glucose or UDP-*N*-acetyl-D-glucosamine; UDP-D-ManNAc, UDP-2-acetamido-2-deoxy-D-mannose or UDP-*N*-acetyl-D-mannosamine; UDP-D-TalNAc, 2-acetamido-2,6-dideoxy-L-talose.

resistance to antibiotics; the first documented case of a vancomycin-resistant *S. aureus* infection in a United States patient was recently reported by the Centers for Disease Control (60).

L-FucNAc has thus far been described exclusively as a constituent of bacterial polysaccharide structures. It is part of the O antigen of *P. aeruginosa* serotypes O4, O11, and O12, of the CP of *S. aureus* serotypes 5 and 8, and of *Streptococcus pneumoniae* CP type 4 (9–12). LPSs of *Escherichia coli* O26 and CP of *Bacteroides fragilis* also contain L-FucNAc (13, 14). It should be noted that not all L-FucNAc-containing bacteria are listed above; for the scope of this study, only those bacteria for which sequence data of the corresponding polysaccharide biosynthesis gene clusters are available have been taken into consideration (*E. coli* O26 polysaccharide cluster data are referred to in Ref. 15). With respect to *P. aeruginosa*, the L-FucNAc-containing strains, particularly International Antigenic Typing System O4 and O11, belong to the most clinically prevalent strains besides serotypes O3 and O6 (16). The O11 strain PA103 is a high level exotoxin A producer (17). *S. aureus* CP serotypes 5 and 8 make up ~80% of clinical isolates (18), and L-FucNAc is a component of both CP structures. Moreover, both *P. aeruginosa* and *S. aureus* are associated with nosocomial infections, as well as being known for resistance against antibiotics. *S. pneumoniae* type 4 capsule is a component of a heptavalent streptococcal vaccine, which is available commercially (19). These data implicate the importance of the L-FucNAc residue in pathogenicity. Targeting its biosynthesis could lead to the development of therapeutic agents that affect important virulence factors of Gram-positive and Gram-negative bacteria.

To date, the biosynthesis pathway leading to the nucleotide-activated precursor of L-FucNAc is not clearly defined. Two putative pathways have been proposed, both lacking any experimental evidence. Lee and Lee (20) suggested a three-step route starting from UDP-D-ManNAc and involving (i) 3-epimerization, (ii) 5-epimerization, and (iii) 6-dehydration leading to UDP-L-FucNAc. Jiang *et al.* (15) proposed a reaction scheme analogous to the biosynthesis of GDP-L-fucose from GDP-D-mannose. This group suggested that UDP-D-GlcNAc is first converted to UDP-D-ManNAc to get the same precursor as in the above pathway. The next reaction step is 4,6-dehydration to get UDP-2-acetamido-2,6-dideoxy-D-*lyxo*-4-hexulose, and finally a bifunctional enzyme would catalyze 3,5-epimerization and 4-reduction to yield UDP-L-FucNAc. The *S. aureus* genes *cap5I8E*, *cap5I8F*, and *cap5I8G* or the homologous *S. pneumoniae* genes *cps4M(J)*, *cps4N(K)*, and *cps4L* have been proposed to be involved in this biosynthesis (15, 20).

We present for the first time a proposed biosynthetic pathway for nucleotide-activated L-FucNAc, namely UDP-L-FucNAc from its precursor UDP-D-GlcNAc. We provide evidence that three *P. aeruginosa* enzymes, WbjB, WbjC, and WbjD (and their *S. aureus* homologs Cap5E, Cap5F, and Cap5G) catalyze a five-step reaction cascade.

EXPERIMENTAL PROCEDURES

Materials—UDP-*N*-acetyl-D-glucosamine, UDP-*N*-acetyl-D-galactosamine, UDP-D-glucose, NAD^+, NADH, $NADP^+$, NADPH, and the antibiotics used in this study were obtained from Sigma-Aldrich. HiTrap Chelating columns were purchased from Amersham Biosciences, Econo-Pac High Q columns were from Bio-Rad, and pET28a, pET24a+, and pET24c+ were from Novagen (Madison, WI).

Bacterial Strains, Cloning Vectors, and Growth Conditions—The bacterial strains and plasmids used in this study are listed in Table I. *P. aeruginosa* strains were grown in Luria broth (Invitrogen) or on *Pseudomonas* Isolation Agar (Difco Laboratories, Detroit, MI). *S. aureus* was grown in tryptic soy broth (Difco Laboratories). *E. coli* strains Top10 (Invitrogen) and JM109 (21) were used for plasmid propagation. *E. coli* strain SM10 (22) was used as donor in bacterial conjugation. For protein overexpression *E. coli* strain BL21(DE3) was used (Novagen). Overexpression was induced by the addition of isopropyl-1-thio-β-D-galactopyranoside (Invitrogen) at a final concentration of 1 mM. The media were supplemented with ampicillin (100–250 μg/ml), kanamycin (25 μg/ml or 50 μg/ml), carbenicillin (250 μg/ml for *E. coli* and 300 μg/ml for *P. aeruginosa*), gentamicin (15 μg/ml for *E. coli* and 300 μg/ml for *P. aeruginosa*), tetracycline (15 μg/ml for *E. coli* and 100 μg/ml for *P. aeruginosa*), chloramphenicol (10 μg/ml), or erythromycin (10 μg/ml) when necessary.

Analytical Techniques—SDS-PAGE was done according to the method of Laemmli (23) with slight modifications. Gels were stained with Coomassie Brilliant Blue R-250 (Sigma-Aldrich). The protein concentrations were determined as described by Bradford (24). LPS was prepared according to the method of Hitchcock and Brown (25). The samples were run on a 12% SDS-PAGE gel, and the LPS was either transferred to a nitrocellulose membrane or visualized by a rapid silver staining procedure (26). Antibodies MF55-1 (mAb to B-band O antigen of serotype O11) (27), grouping antiserum O11 (polyclonal antibody to B-band O antigen of serotype O11; Chengdu Institute of Biological Products, Chengdu, China), and N1F10 (mAb to A-band O antigen) (28) were used for Western immunoblotting analysis. The blots were developed with anti-mouse immunoglobulin G alkaline phosphatase (Jackson Immunoresearch, West Grove, PA) for mAbs, and anti-rabbit immunoglobulin G alkaline phosphatase (Bio-Rad) for the polyclonal antiserum. 5-Bromo-4-chloro-3-indolyl phosphate and nitroblue tetrazolium (Sigma-Aldrich) were used as the alkaline phosphatase substrate.

Colony immunoblot analysis was performed as previously described (29) with the use of CP5-specific polyclonal rabbit antiserum. The blots were developed using protein A-horseradish peroxidase conjugate (Zymed Laboratories Inc., South San Francisco, CA) and the Bio-Rad horseradish peroxidase conjugate substrate kit.

Sequence Analysis—BLAST (30) and Multalin (31) were used for analysis of nucleotide and protein sequences.

DNA Manipulations, PCR, DNA Sequencing, and Protein Sequencing—All of the standard DNA recombinant procedures were performed according to the methods described by Sambrook *et al.* (32) or as recommended by the corresponding manufacturer. PCR was carried out with a GeneAmp PCR System 2400 (PerkinElmer Life Sciences). DNA sequencing was performed by Mobix Lab (Hamilton, Canada) or by the Beth Israel Deaconess Molecular Medicine Unit (Boston, MA). N-terminal protein sequencing was performed by the Dana Farber Molecular Biology Core Facility (Boston, MA).

Plasmid Construction—The oligonucleotide primer sequences are given in Table II. Chromosomal DNA of *P. aeruginosa* International Antigenic Typing System strain O11 or *S. aureus* capsular type 5 was used for amplification of the genes. Pwo polymerase (Roche Molecular Biochemicals) was used for PCR amplification. Primer pairs wbjB1F/wbjB2R, wbjC1F/wbjC2R, wbjD1F/wbjD2R, and capE1F/capE2R were used for amplification of the *wbjB*, *wbjC*, *wbjD*, and *cap5E* (clinical isolate provided by A. Chow, Vancouver, Canada) genes, respectively. The PCR products of genes *wbjD* and *cap5E* were digested with *Nco*I and *Bam*HI and ligated into the modified pET23 derivative (33), cut with the same enzymes. PCR product *wbjC* was cut with *Nde*I and *Hin*dIII and ligated into appropriately digested pET28a. Finally, PCR product *wbjB* was digested with *Nde*I and *Eco*RI and ligated into *Nde*I/*Eco*RI-cut pET28a. The corresponding plasmids pFuc11 (*wbjB*), pFuc12 (*wbjC*), pFuc13 (*wbjD*), and pFuc21 (*cap5E*) were confirmed by DNA sequencing and used for amplification of PCR products for complementation studies and/or overexpression of N-terminal histidine-tagged fusion proteins.

S. aureus cap5E, *capF*, and *capG* genes were PCR-amplified from strain Newman chromosomal DNA with High Fidelity PCR Supermix (Invitrogen). Primers 5E-F and 5E-R were utilized to amplify the *cap5E* gene. This amplicon was digested with *Xho*I and *Nhe*I and ligated to pET24a+ digested with the same enzymes. The resultant plasmid pKBK50d contained the ribosomal-binding site and the ATG start site of the pET vector in-frame with the entire *cap5E* gene and C-terminal six-histidine tag. A similar strategy was applied to clone the *cap5F* gene; it was amplified with primers 5F-F and 5F-R and cloned into the pET24a+ vector, creating plasmid pET5F1.1. The *cap5G* gene was amplified with KK1 and KK2. The 1.18-kb amplicon was digested with *Xba*I and *Eco*RI and ligated to appropriately digested pET24c+, yielding plasmid pKBK6a with a C-terminal histidine tag. All of the plasmids were confirmed by nucleotide sequencing of the PCR-amplified genes.

To construct the plasmids containing a nonpolar gene disruption of *P. aeruginosa wbjB*, the PCR product described above was ligated into *Sma*I-cut pEX100T, taking advantage of the blunt-end PCR product made by Pwo polymerase. The *wbjB*-containing plasmid pKOB1 was

TABLE I
Bacterial strains and plasmids used in this study

	Genotype/description	Source
Strains		
E. coli		
Top10	F$^-$ *mcrA* Δ(*mrr-hsd*RMS-*mcr*BC) ϕ80*lac*ZΔM15 Δ*lac*X74 *deo*R *rec*A1 *ara*D139 Δ(*ara*A-*leu*)7697 *gal*U *gal* K *rps*L (Str^R) *end*A1 *nup*G	Invitrogen
JM109	*end*A1 *rec*A1 *gyr*A96 *thi hsd*R17 (r_k^-,m_k^+) *rel*A1 *sup*E44 λ$^-$ Δ(*lac-pro*AB) [F′ *tra*D36 *pro*AB *laq*IqZΔM15	Ref. 21
SM10	*thi-1 thr leu ton*A *lac*Y *sup*E *rec*A RP4–2-Tc::Mu, Km^r	Ref. 22
BL21(DE3)	*E. coli* B F$^-$ *dcm ompT hsdS*(r_B^- m_B^-) *gal* λ(DE3)	Novagen
P. aeruginosa		
IATS O11	Wild-type strain serotype O11 (ATCC 33358)	ATCC
PA103	Wild-type strain serotype O11	Ref. 52
BK103B	PA103 with *wbj*B::*aacC1* mutation	This study
S. aureus		
VI-114	Capsular serotype 5 strain	A. W. Chow (University of British Columbia)
Newman	CP5-positive	NCTC 8178
G01	Newman with *ermB*-inactivated *cap5G* gene	This study
F4	Newman with *ermB*-inactivated *cap5F* gene	This study
RN4220	CP-negative, restriction-negative	Ref. 53
8325–4	NCTC 8325 cured of prophages; CP-negative	Ref. 54
Plasmids		
pET23der	Expression vector for histidine fusion	Ref. 33
pET28a	Expression vector for histidine fusion	Novagen
pET24a+	Expression vector for histidine fusion	Novagen
pET24c+	Expression vector for histidine fusion	Novagen
pEX100T	Conjugation vector with *bla* and *sacB* genes	Ref. 36
pUCGm	pUC derivative containing *aacC1* gene	Ref. 55
pUCP27	*E. coli* and *P. aeruginosa* shuttle plasmid for gene complementation	Ref. 56
pFuc11	*wbjB* in pET28a (*Nde*I/*Eco*RI)	This study
pFuc12	*wbjC* in pET28a (*Nde*I/*Hin*dIII)	This study
pFuc13	*wbjD* in pET23der (*Nco*I/*Bam*HI)	This study
pFuc21	*cap5E* in pET23der (*Nco*I/*Bam*HI)	This study
pKOB1	*wbjB* in pEX100T (*Sma*I)	This study
pKOB2	Insertion of *aacC1* in *wbjB* of pKOB1 (*Kpn*I)	This study
pPAB27	*wbjB* in pUCP26 (*Xba*I/*Eco*RI)	This study
pSAE27	*cap5E* in pUCP26 (*Xba*I/*Kpn*I)	This study
pKBK50d	*cap5E* in pET24a+ (*Xho*I/*Nhe*I)	This study
pET5F1.1	*cap5F* in pET24a+ (*Xho*I/*Nhe*I)	This study
pKBK6a	*cap5G* in pET24a+ (*Xba*I/*Eco*RI)	This study
pJCL69	Subclone of *cap5* (contains intact *capF* through *capH*) in pGEM-7Zf+	Ref. 57
pJCL69–2	294-bp *Bcl*I fragment deleted from *cap5G* in pJCL69	This study
pERMB	*ermB* cassette (from Tn551) in pGEM7Zf+	Ref. 39
pJCL69–2ermB	1.3-kb *ermB* fragment (*Bam*HI/*Bcl*I) from pERMB in pJCL69–2	This study
pCL10	*E. coli*/*S. aureus* temperature-sensitive shuttle vector	Ref. 58
pKOR1	4.4-kb *Xba*I/*Bam*HI fragment from pJCL69–2ermB in pCL10	This study
pAP1.2EX	pCL10 containing *ermB* cassette	This study
pKOR3	1.6-kb amplicon (*cap5G* and 450 bp of *cap5F*) in pAP1.2EX (XbaI)	This study
pKOR4	1.9-kb amplicon (385 of bp *cap5D, cap5E* and 530 bp *cap5F*) in pKOR3 (*Sac*I/*Eco*RV)	This study
pLI50	*E. coli*/*S. aureus* shuttle vector	Ref. 59
pJCL43	2.2-kb *cap5* subclone in pGEM7Zf+ (contains *cap5G*)	Ref. 57
pKOR2	2.2-kb *Bam*HI/*Xba*I fragment of pJCL43 carrying *cap5G* in pLI50	This study
pCAP16	Subclone of *cap5* locus in pCU1; contains *cap5A* through *cap5E*	Ref. 44
pCAP17	Subclone of *cap5* locus in pCU1; contains *cap5A* through *cap5F*	T. Foster (Ireland)

subsequently cut with *Kpn*I, and the *aacC1* gene (gentamicin resistance cassette) from pUCGm was ligated into pKOB1 to yield the *wbjB* knockout plasmid pKOB2.

To create a plasmid for *S. aureus cap5G* gene disruption, subclone pJCL69 (containing the end of *cap5E* through the start of *cap5I*) was digested with *Bcl*I, releasing a 294-bp fragment 50 bp downstream of the ATG start site of *cap5G* yielding pJCL69-2. The *ermB* gene from pERMB was ligated into the *Bcl*I site of pJCL69-2 to create pJCL69-2ermB. A 4402-bp *Xba*I-*Bam*HI fragment from pJCL69-2ermB was ligated to digested pCL10 to yield pKOR1. To create a knockout plasmid for use in *cap5F* allelic replacement, a modified pCL10 plasmid containing *ermB* in the *Bam*HI site was constructed (pAP1.2EX). A 1.6-kb region of the *cap*5 gene locus (containing 450 bp of *cap5F* gene and 1124 bp of the *cap5G* gene) was PCR-amplified using primers 12402F2 and 12402R2, digested with *Xba*I, and ligated to *Xba*I-digested pAP1.2EX to form pKOR3. A 1941-bp region of the *cap5* locus containing 385 bp of *cap5D*, the complete open reading frame (1026 bp) of *cap5E* gene, and 530 bp of *cap5F* was PCR-amplified using primers 12402F1 and 12402R1. This amplicon was digested with *Sac*I and *Eco*RV and ligated to similarly digested pKOR3 to yield the 11.32-kb plasmid pKOR4.

pFuc11 and pFuc21 plasmid DNA was used to amplify the genes for the complementation plasmids. PCR was carried out with T7 forward primer and the corresponding reverse primers used to get the expression plasmids. The *Xba*I site in the T7 promoter sequence was used to ligate the PCR product into pUCP27 digested with *Xba*I/*Eco*RI for *wbjB* or *Xba*I/*Kpn*I in the case of *cap5E*. Thus, we could take advantage of the ribosomal-binding site of the pET vectors and achieve complementation with the N-terminally histidine-tagged fusion proteins. The resulting plasmids pPAB27 and pSAE27 were confirmed by DNA sequencing. *S. aureus* plasmid pKOR2 was constructed by ligating a 2.2-kb *Bam*HI-*Xba*I fragment from pJCL43 containing the *cap5G* gene along with 920 bp of upstream and 144 bp of downstream flanking sequences into the *E. coli*/*S. aureus* shuttle vector pLI50.

Protein Overexpression and Purification—Expressions were carried out at 37 °C using terrific broth (32), supplemented with 50 μg/ml kanamycin for WbjB and WbjC, with 25 μg/ml kanamycin for Cap5E, Cap5F, or Cap5G, or with 250 μg/ml ampicillin for WbjD. The cultures were grown to an $A_{600\ nm}$ of 0.6, and expression was induced with isopropyl-1-thio-β-D-galactopyranoside at a final concentration of 1 mM. WbjB ,WbjD, Cap5E, and Cap5F expression was carried out for 3 h at 37 °C, WbjC was expressed for 4 h at 37 °C, and Cap5G was expressed for 4 h at 30 °C. The cells were disrupted on ice by ultrasonication. Cell debris and membrane fractions were removed by ultracentrifugation at 300,000 × *g*. Purifications using nickel chelating columns were per-

TABLE II
Oligonucleotide primers used in this study

Primer[a]	Primer sequence[b]
wbjB1F (+)	5′-GGACTCGAGCATATGGATAAGAACTCTGTTC-3′
wbjB2R (−)	5′-GGAATTCAGTTACAAGAACTTTCATCG-3′
wbjC1F (+)	5′-GTAGATCTCATATGAAAGTTCTTGTAACTG-3′
wbjC2R (−)	5′-GACAAGCTTCTCACTATACCTTACGCACC-3′
wbjD1F (+)	5′-CGAGATCTACCATGGAGAAGCTAAAAGTCG-3′
wbjD2R (−)	5′-GAGAATTCGGATCCTTGCCATCAACTCC-3′
wzy11F (+)	5′-GTTATGGTTCGATCTATATGG-3′
cap5E1F (+)	5′-GCAGAGCTCCATGGTCGATGACAAAATTTTAT-3′
cap5E2R (−)	5′-TGGGATCCGGTACCTCTCCTATCTCATTGAAGC-3′
T7 (+)	5′-TAATACGACTCACTATAGGG-3′
gent1F (+)	5′-GTTAGGTGGCTCAAGTATGG-3′
gent2R (−)	5′-AGATCACATAAGCACCAAGC-3′
KKI (+)	5′-ACAATCTAGAGCCAGATACGTATTTCTTGG-3′
KK2 (−)	5′-ACAAGAATTCCATTTCCTCCAAGTATTTCG-3′
5E-F (+)	5′-GGAGGCTAGCATGTTCGATGACAAAATT-3′
5E-R (−)	5′-CTCTCGAGTCTCATTGAAGCTTTATAAT-3′
5F-F (−)	5′-GATAGGCTAGCTTGACGTTGAAT-3′
5F-R (−)	5′-TCCATGCGCTCGAGCTCCAAGA-3′
12402F1 (+)	5′-GCATGAGCTCAAGGTGGCGAAGTATT-3′
12402R2 (−)	5′-TGGAGTTCCTTCAATAGCACGCTTTA-3′
12402F2 (+)	5′-CAGTCTAGACTCGATCGAACATTGCC-3′
12402R2 (−)	5′-TTATCTAGACAATCGCTATCCTCATC-3′

[a] Forward and reverse primers are represented by plus and minus signs, respectively.
[b] The underlined sequences represent the restriction sites used to clone the PCR products.

formed as recommended by the manufacturers. Purified WbjC and WbjD could be obtained at 200 mM imidazole, whereas WbjB, Cap5E, Cap5F, and Cap5G were eluted from the column at 300 mM imidazole. Dithiothreitol was added to a final concentration of 1 mM, and the proteins were stored at −20 °C after the addition of 40% glycerol. The purity of the enzymes was checked by SDS-PAGE analysis on a 10% gel, and N-terminal protein sequencing was performed on Cap5E, Cap5F, and Cap5G to verify the purified proteins.

Capillary Electrophoresis (CE) Analysis of UDP-L-FucNAc Biosynthesis—CE analysis was performed with a P/ACE MDQ Glycoprotein system with UV detection (Beckman Coulter, Fullerton, CA). The samples were separated at 22 kV in 25 mM borate buffer (pH 9.5) at 25 °C. Typically, the reactions contained 0.5 mM UDP-D-GlcNAc, 0.1 mM $NADP^+$, and an excess of hydride donor (NADH or NADPH). For CE-MS analysis, the UDP-D-GlcNAc concentration was 0.1 or 0.5 mM. The standard reaction buffer was 20 mM Tris-HCl at pH 8.0 supplemented with 10 mM $MgCl_2$. The enzymes (~1 μg each) were added, and the reaction mixtures were incubated at 37 °C for 60 min before being analyzed by CE. The reaction cascades were investigated as stepwise reactions adding one enzyme at a time (allowing optimal substrate conversion on each reaction step) and as combined reactions adding more than one enzyme to start the reaction.

Coupled CE-MS Analysis of UDP-L-FucNAc Biosynthesis—The crystal model 310 CE instrument (ATI Unicam, Boston, MA) was coupled to an API 3000 mass spectrometer (MDS/Sciex, Concord, Canada) via a micro Ionspray interface. A sheath solution (isopropanol:methanol, 2:1) was delivered at a flow rate of 1 nl/min to a low dead volume tee (internal diameter, 250 μm; Chromatographic Specialties, Brockville, Canada).

The separation was achieved using a 90-cm bare fused silica capillary with a buffer of 30 mM morpholine/formic acid in deionized water, pH 9.0, with 5% methanol. For positive detection mode, a 10 mM ammonium acetate buffer, pH 9.0, containing 5% methanol was used. A separation voltage of 30 kV was typically applied at the injection end of the capillary. The outlet of the capillary was tapered to a ~15-μm diameter with a laser puller (Sutter Instruments, Novato, CA).

Mass spectra were acquired using a dwell time of 3.0 ms/step of 1 *m/z* unit in full mass scan mode. For CE-MS/MS experiments, a sample loading of ~25 nl was applied. The MS/MS data were acquired with dwell times of 3.0 ms/step of 1 *m/z* unit on the triple quadrupole instrument. Collisional activation of selected precursor ions in the radiofrequency-only quadrupole collision cell was achieved using nitrogen as a target gas. Further information was obtained by conducting MS/MS experiments on the second generation fragment ions (or MS/MS/MS), promoted by front end collision-induced dissociation. These selected ions were formed by increasing the orifice voltage (from 60 to 180 V, in this case).

Synthesis and Preparation of Intermediate Products—5.5 μmol (3.5 mg) of UDP-D-GlcNAc were converted quantitatively to a mixture of keto-sugars using 100 μg of WbjB. The reaction was carried out in 20 mM triethylammonium bicarbonate buffer (pH 8.0) for 4.5 h at 37 °C. The protein was removed by ultrafiltration with Centriplus cartridges (Millipore, Bedford, MA). For analysis of the keto-mixture, the sample was acidified to pH 4.5 with Dowex 50 (Bio-Rad) to get rid of CO_2 and concentrated to 100 μl by lyophilization. This concentrated compound was analyzed by NMR. The keto-sugar that migrated faster than $NADP^+$, as judged by CE analysis, was purified over an Econo-Pac High Q anion exchange column with a linear triethylammonium bicarbonate gradient (0–500 mM). Fractions containing the keto-sugar were pooled, acidified with Dowex 50, lyophilized completely, and analyzed by NMR.

5.5 μmol (3.5 mg) of UDP-D-GlcNAc were converted quantitatively to the putative UDP-2-acetamido-2,6-dideoxy-L-talose using 200 μg each of WbjB and WbjC and equimolar amounts of NADPH. The reaction was performed overnight in 20 mM Tris buffer (pH 8.0) at 37 °C. The enzyme from the reaction mix was removed by ultrafiltration with Centriplus cartridges. The purification of the reaction product was performed as described above for the keto-intermediate. The fractions corresponding to UDP-2-acetamido-2,6-dideoxy-L-talose were pooled, acidified to pH 4.5 with Dowex 50, concentrated to a final volume of 80 μl by lyophilization, and used for NMR analysis. The yield was ~3 mg of UDP-2-acetamido-2,6-dideoxy-L-talose (85%).

NMR Analysis of Intermediate Products—All of the spectra were acquired using a Varian Inova 500 MHz spectrometer equipped with a Z-gradient 3-mm triple resonance (^1H, ^{13}C, ^{31}P) probe. The lyophilized UDP-*xylo*-sugar sample was dissolved in 140 μl of 99% D_2O. The other samples, dissolved in 80–100 μl of H_2O, were prepared by adding D_2O up to a volume of 140 μl. The experiments were performed at 25 °C with suppression of the deuterated H_2O signal at 4.78 ppm. The methyl resonance of acetone was used as an internal or external reference at 2.225 ppm for ^1H spectra and 31.07 ppm for ^{13}C spectra. Standard homo- and heteronuclear correlated two-dimensional pulse sequences from Varian, COSY, HSQC, HMBC, and ^{31}P HMQC were used for general assignments (34). Selective one-dimensional TOCSY with a Z-filter and one-dimensional NOESY experiments were performed for complete residue assignment and for the determination of ^1H-^1H nuclear Overhauser enhancements (35). A mixing time of 80 ms was used for the one-dimensional TOCSY experiments and 800 ms for the one-dimensional NOESY experiments.

Nonpolar Gene Knockout of wbjB—The *wbjB*::*aacC1*-containing plasmid pKOB2 was transformed into the mobilizing *E. coli* strain SM10, and the construction of the *wbjB* knockout mutant was accomplished as was described by Schweizer and Hoang (36). Gene replacement was confirmed by resistance to gentamicin, resistance to sucrose, susceptibility to carbenicillin, and PCR. Primer pairs wbjB1F/wbjB2R, wbjB1F/wbjC2R, wbjB1F/gent2R, gent1F/wbjB2R, and wzy11F/wbjB2R (Table II) were used to prove nonpolar insertion of the *aacC1* gene into the B-band O antigen locus. wzy11F is a forward primer homologous to sequence located directly upstream of *wbjB*, and gent1F and gent2R are forward and reverse primers within the gentamicin resistance gene *aacC1*. Western immunoblotting analysis provided further evidence of the successful mutation of the gene.

Complementation of the wbjB Gene Knockout—The plasmids pPAB27 and pSAE27, which have the *wbjB* or *cap5E* in the opposite direction as the *lac* promoter (resulting in lower expression levels of the cloned genes), were transformed into the knockout strain BK103B by electroporation. The cultures were grown overnight, and LPS was analyzed by methods described above.

Nonpolar Gene Knockout of capF and capG—Plasmids pKOR1 and pKOR4 were separately electroporated into *S. aureus* RN4220 (37) and transduced with phage 80α (38) into *S. aureus* Newman, in both cases selecting for Cm^r colonies at 30 °C. Allelic replacements were performed as described by Kiser *et al.* (39). Southern blot analysis confirmed the identity of *cap5G* mutant G01 and cap5F mutant F4. Colony immunoblot analysis of CP5 expression was performed as previously described (29).

Complementation of the cap5G and cap5F Gene Knockouts—Plasmid pKOR2 carrying *cap5G* was transformed into *S. aureus* RN4220 and then transduced into *S. aureus* Newman G01. The *S. aureus* vector pLI50 was similarly introduced into strain G01 as a control. The *cap5F* knockout mutant (strain F4) was complemented *in trans* with pCAP17, a plasmid containing the *cap5* promoter region and intact *cap5A* through *cap5F* in pCUI. pCAP16, a similar pCU1 construct containing the *cap5* promoter and *cap5A* through *cap5E*, was utilized as a negative control.

TABLE III
Enzymes involved in UDP-L-FucNAc biosynthesis

Bacterial strain	Proteins encoded by three contiguous genes in the different bacteria (accession numbers)[a]		
P. aeruginosa PA103	WbjB (AAD45265)	WbjC (AAD45266)	WbjD (AAD45267)
P. aeruginosa IATS O17	WbjB (AAF72954)	WbjC (AAF72955)	WbjD (AAF72956)
P. aeruginosa IATS O4	ORF 9 (AAM27785)	ORF 10 (AAM27786)	ORF 11 (AAM27787)
P. aeruginosa IATS O11	ORF 8 (AAM27575)	ORF 9 (AAM27576)	ORF 10 (AAM27577)
P. aeruginosa IATS O12	ORF 20 (AAM27601)	ORF 21 (AAM27602)	ORF 22 (AAM27603)
S. aureus Reynolds/Newman	Cap5E (AAC46088)	Cap5F (AAC46089)	Cap5G (AAC46090)
S. aureus Becker	Cap8E (AAB49434	Cap8F (AAB49435)	Cap8G (AAB49436)
S. pneumoniae TIGR4	Cps4M (J) (AAK74531)	Cps4N (K) (AAK74532)	Cps4O (AAK74533)
S. pneumoniae WCH34	Fnl1/ORF13 (AAK20678)	Fnl2/ORF14 (AAK20679)	Fnl3/ORF15 (AAK20680)
B. fragilis 638R	WcgJ (AAD56742)	WcgK (AAD56743)	WcgL (AAD56744)
P. multocida PM70	WbjB (AAK03091)	WbjC (AAK03092)	WbjD (AAK03093)
L. interrogans Copenhageni	ORFC10 (AAK19906)	ORFC32 (AAK19897)	ORFC11 (AAK19898)
L. interrogans Pomona	ORFP10 (AAL49416)	ORFP32 (AAL49417)	ORFP11 (AAL49418)

[a]Proteins appearing in the same column of this table are highly homologous to each other.

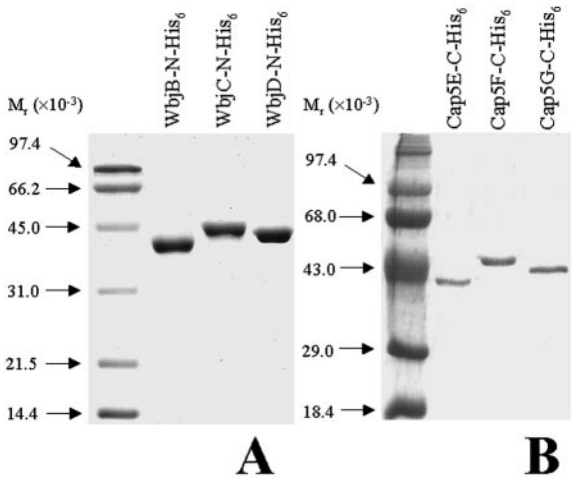

FIG. 1. **SDS-PAGE analysis of purified UDP-L-FucNAc biosynthesis enzymes.** *A*, *P. aeruginosa* International Antigenic Typing System O11. *B*, *S. aureus* serotype 5. His_6 refers to the hexahistidine tag at the N or C terminus. Prestained protein molecular weight standards (Invitrogen) or the Low Range SDS-PAGE Molecular Weight Standard (Bio-Rad) were used.

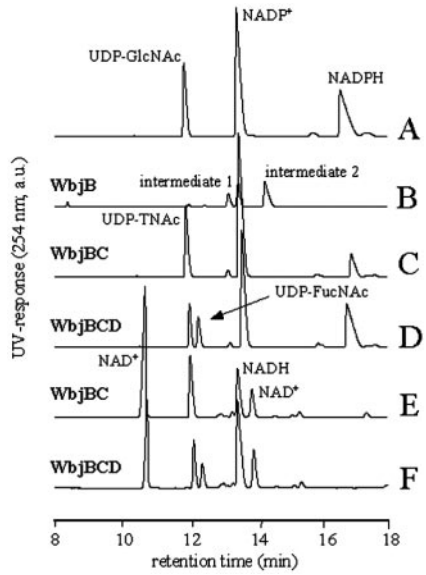

FIG. 2. **CE analysis of UDP-L-FucNAc biosynthesis.** *A*, standard, UDP-D-GlcNAc, $NADP^+$, and NADPH. *B*, UDP-D-GlcNAc, converted with WbjB and $NADP^+$ (*intermediates 1* and *2* represent the two 2-amino-4-keto-2,6-dideoxy-hexose intermediates). *C*, UDP-D-GlcNAc, converted with WbjB, WbjC, $NADP^+$, and NADPH (*UDP-TNAc* refers to UDP-2-acetamido-2,6-dideoxy-L-talose). *D*, UDP-D-GlcNAc, converted with WbjB, WbjC, WbjD, $NADP^+$, and NADPH. *E*, UDP-D-GlcNAc, converted with WbjB, WbjC, $NADP^+$, and NADH (NAD^+ and NADH have not been added to the standard *A*; the reason being that NADH comigrates with $NADP^+$, and NAD^+ results in two peaks). *F*, UDP-D-GlcNAc, converted with WbjB, WbjC, WbjD, $NADP^+$, and NADH. *a.u.*, arbitrary units.

RESULTS

Sequence Analyses—A common feature of bacterial gene clusters associated with the biosynthesis of L-FucNAc is the presence of three consecutive genes with no assigned function (Table III). These genes are also part of the genomes of *Pasteurella multocida* PM70 and *Leptospira interrogans* serovars Copenhageni and Pomona. Whether these two bacteria contain L-FucNAc in their surface polysaccharide is not known. The proteins encoded by *wbjB/cap5E* and *wbjC/cap5F* or their homologs belong to the SDR protein family (40). Both WbjB/Cap5E and WbjC/Cap5F have the nucleotide-binding signature G*XX*G*XX*G near their N terminus (referred to as the Rossmann fold) essential for binding of the cofactor NAD^+ or $NADP^+$ (41). Another typical feature of the SDR protein family is the so-called catalytic triad, SMK in the case of WbjB/Cap5E and SYK in WbjC/Cap5F. WbjB/Cap5E is moderately homologous to WbpM, which is putatively involved in UDP-*N*-acetyl-D-fucosamine/quinovosamine biosynthesis and shows reactivity on UDP-D-GlcNAc (42). Thus, we postulated WbjB/Cap5E to be the enzyme catalyzing the first reaction step involving UDP-D-GlcNAc. Because proteins of this family are highly homologous, is very difficult to predict their exact function. The third putative L-FucNAc biosynthesis protein is WbjD/Cap5G, which shows homology to UDP-GlcNAc 2-epimerases involved in the biosynthesis of UDP-D-ManNAc (39). To determine whether the gene products of *wbjB/cap5E*, *wbjC/cap5F*, and *wbjD/cap5G* are actually involved in the biosynthesis of nucleotide-activated L-FucNAc and to determine the order in which they would act in the pathway, two approaches have been used: overexpression of the corresponding proteins to carry out *in vitro* enzyme assays and knocking out the genes, evaluating the phenotype of the mutants, and performing complementation studies.

Expression and Purification of the UDP-L-FucNAc Biosynthesis Enzymes—WbjB, WbjC, WbjD, Cap5E, and Cap5F were expressed at high levels at 37 °C. High level expression resulting in soluble Cap5G could only be achieved at 30 °C. After sonication and ultracentrifugation, the majority of the proteins proved to be in the supernatant, enabling high yield affinity purification on chelating columns. After addition of 40% glycerol, the enzymes were stable at −20 °C for several weeks. The apparent molecular masses (M_r) of the proteins, determined by SDS-PAGE, were in good agreement with the calculated molecular masses, *i.e.* WbjB, 40.7 kDa; WbjC, 43.6 kDa; and WbjD, 43.9 kDa (Fig. 1*A*). Purified recombinant Cap5E, Cap5F, and Cap5G are shown in Fig. 1*B*. The predicted molecular masses

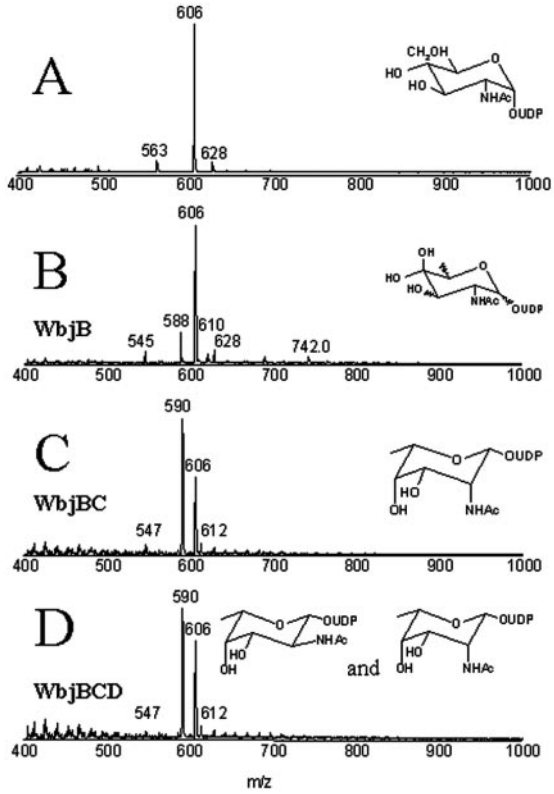

FIG. 3. **CE-MS analysis of UDP-L-FucNAc biosynthesis in the negative mode.** *A*, UDP-D-GlcNAc. *B*, UDP-D-GlcNAc, converted with WbjB and $NADP^+$. *C*, UDP-D-GlcNAc, converted with WbjB, WbjC, $NADP^+$, and NADPH. *D*, UDP-D-GlcNAc, converted with WbjB, WbjC, WbjD, $NADP^+$, and NADPH. Peaks at *m/z* 563, 545, and 547 are due to the UDP moiety. The peak at *m/z* 742 results from $NADP^+$, and the peaks at *m/z* 610, 612, and 628 are due to mono-sodium salts of *m/z* 588, 590, and 606, respectively.

of these recombinant proteins are 39.9, 43.7, and 45.1 kDa, respectively. N-terminal protein sequencing of Cap5E (MFDDKILL), Cap5F (LTLNIVIT), and Cap5G (MEKLKLMTIV) correlated with the predicted initial eight to ten amino acids for these proteins. The purified proteins were used for functional characterization of the biosynthesis pathway of nucleotide-activated L-FucNAc.

WbjB/Cap5E Is a Trifunctional Enzyme Catalyzing the First Three Enzymatic Reactions—Sequence analysis suggested that WbjB was the first enzyme in the pathway with UDP-D-GlcNAc as substrate. Indeed, in the WbjB enzyme-substrate reaction, the peak corresponding to UDP-D-GlcNAc disappeared almost completely, and two new peaks appeared on CE analysis (Fig. 2*B*). $NADP^+$ was an essential cofactor in WbjB catalysis. Addition of NAD^+ or the absence of any added cofactor resulted in less than 5% substrate conversion. Despite performing time course experiments to determine which of the two peaks appeared first, it was not possible to make any assignment. Both products were formed simultaneously in a 1:3 ratio (Fig. 2*B*, *intermediates 1* and *2*). The achieving of an equilibrium would be characteristic of an epimerase reaction. Two other related sugar nucleotides, UDP-*N*-acetyl-D-galactosamine and UDP-D-glucose, also were tested as substrates with WbjB and cofactor, but no reaction could be detected. To further verify that WbjB is the enzyme catalyzing the first reaction step, purified WbjC or WbjD were also incubated with UDP-D-GlcNAc; again no substrate conversion was discerned.

CE-MS was used to characterize further the two reaction products formed by WbjB. Although the reaction appeared to be close to quantitative, only a minor part of UDP-D-GlcNAc was converted to a product with a molecular mass of 588 (negative mode; Fig. 3*B*), the expected mass if the first reaction step involved 4,6-dehydration. Table IV lists parent and fragment ions obtained in CE-MS analyses. However, CE-MS/MS in the positive mode at *m/z* 608 clearly demonstrated that the product

TABLE IV
MS analysis of the reaction steps leading to UDP-L-FucNAc (positive mode)

m/z	Assignment
Peaks arising from UDP-D-GlcNAc	
608	UDP-D-GlcNAc parent peak
405	UDP moiety
204	D-GlcNAc moiety
186	D-GlcNAc minus H_2O
168	D-GlcNAc minus $2H_2O$
144	Deacetylated D-GlcNAc minus H_2O
138	D-GlcNAc minus $2H_2O$ and formaldehyde
Peak arising from UDP-2-acetamido-4-keto-2,6-dideoxy sugar in the ketal form	
608	Parent peak
405	UDP moiety
204	Sugar moiety
186	Sugar minus H_2O
168	Sugar minus $2H_2O$
144	Deacetylated sugar minus H_2O
Peak arising from nonhydrated UDP-2-acetamido-4-keto-2,6-dideoxy sugar	
590	Parent peak
405	UDP moiety
186	Sugar moiety
168	Sugar minus H_2O
Peak arising from UDP-2-acetamido-2,6-dideoxy sugars	
592	Parent peak
405	UDP moiety
188	Sugar moiety
170	Sugar minus H_2O
Peaks arising during time course experiment	
204	D-GlcNAc and hydrated 2-acetamido-4-Keto-2,6-dideoxy sugar moiety
186	Either sugar minus H_2O
168	Either sugar minus $2H_2O$
144	Either sugar deacetylated minus H_2O
138	D-GlcNAc minus $2H_2O$ and formaldehyde
126	Either sugar deacetylated minus $2H_2O$

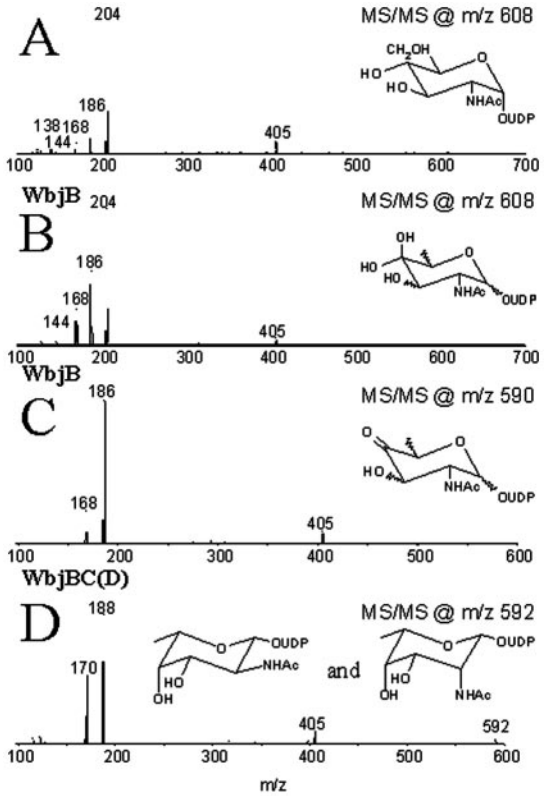

FIG. 4. **CE-MS/MS analysis of UDP-L-FucNAc biosynthesis in the positive mode.** *A*, UDP-D-GlcNAc. *B* and *C*, UDP-D-GlcNAc, converted with WbjB and $NADP^+$. *D*, UDP-D-GlcNAc, converted with WbjB, WbjC, $NADP^+$, and NADPH (UDP-D-GlcNAc, converted with WbjB, WbjC, WbjD, $NADP^+$, and NADPH looks exactly the same as *D*).

formed in the WbjB catalyzed reaction with the same molecular mass as UDP-D-GlcNAc was not UDP-D-GlcNAc (Fig. 4, *A* and *B*). The fragment ion at *m/z* 138 characteristic of *N*-acetylhexose sugars having a hydroxyl group at C-6 disappeared almost completely. A time course experiment was performed to investigate this reaction further. CE-MS/MS/MS was carried out at *m/z* 608 (first generation ions) through *m/z* 204 (second generation ions) to analyze the hexose moiety of the nucleotide-activated sugar. Indeed, a significant decrease of the fragmentation ion at *m/z* 138 was observed (Fig. 5). The presence of a 6-deoxy-sugar with a molecular mass equivalent to that of its parent 6-hydroxy-sugar provided the evidence for the addition of water somewhere on the hexose moiety. CE-MS/MS analysis of the peak at *m/z* 590 (positive mode) demonstrated that the second reaction product is UDP-2-acetamido-4-keto-2,6-dideoxy sugar in the nonhydrated form (Fig. 4*C*). Both CE and CE-MS analyses also were performed using the *S. aureus* homolog Cap5E, with results identical to those obtained for WbjB (data not shown).

To obtain unequivocal evidence of the identity of these intermediates, NMR experiments have been performed. The putative keto-intermediate that migrated faster than $NADP^+$ was purified by anion exchange chromatography. It was lyophilized to dryness and dissolved in D_2O. Although it was fairly unstable, we were able to assign the structure of this intermediate sugar nucleotide; the ^1H spectrum is presented in Figs. 6*A* and 7*A*. One-dimensional selective experiments on the sugar resonances yielded accurate coupling constants. A value of $J_{1,2}$ of 3.6 Hz indicated that H-1 was equatorial, having the α-configuration. A large $J_{2,3}$ value of 10.8 Hz indicated that H-2 and H-3 were *trans* to each other. The strong NOE between H-5 and H-3 indicated that H-3 and H-5 were both axial (Fig. 7*D*). From the HSQC spectrum, the protonated carbons were assigned.

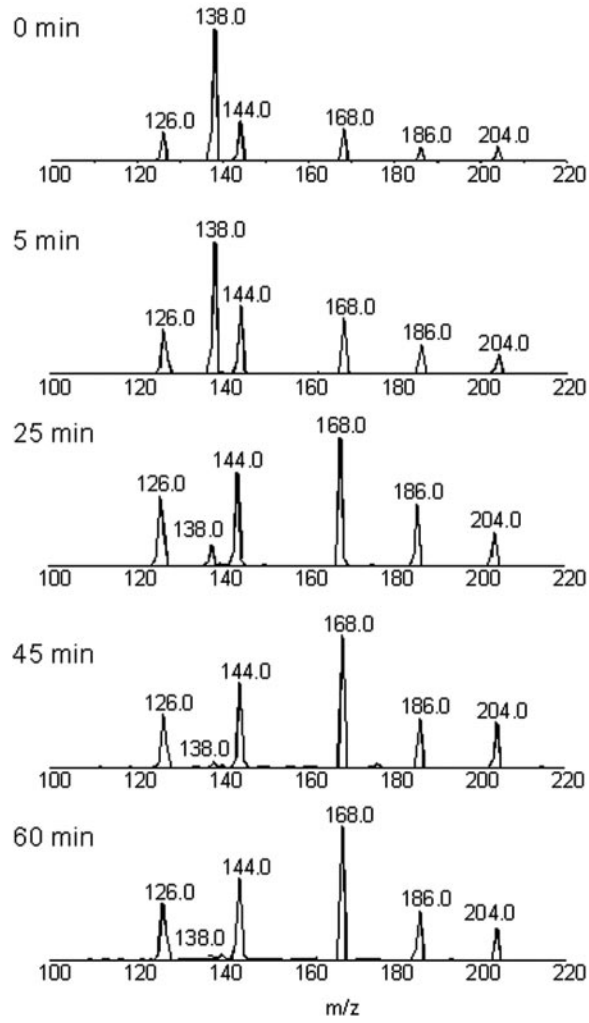

FIG. 5. **Time course investigation of the WbjB-catalyzed reaction using CE-MS/MS/MS analysis in the positive mode.** UDP-D-GlcNAc was reacted with WbjB and $NADP^+$. MS/MS/MS at *m/z* 608 (first generation ions) through *m/z* 204 (second generation ions) was recorded at the time points indicated.

From the HMBC spectrum, the quaternary carbon at C-4 and the NAc-C=O resonances were assigned. Because this sample was dissolved in pure D_2O, the NH resonance was not observed. The chemical shifts of hydrogens and carbons, as well as the ^1H-^1H coupling constants, are given in Table V. The ^1H, ^{13}C, and ^{31}P chemical shifts for the UDP moiety are similar to the one reported before (34). The sugar nucleotide finally arrived at is UDP-2-acetamido-2,6-dideoxy-α-D-*xylo*-4-hexulose.

The second intermediate detected by CE analysis could not be purified in the same manner as the first because of instability. To analyze this sugar, the WbjB reaction mix was concentrated on the lyophilizer after removing the enzyme by ultrafiltration. D_2O was added to the concentrate, and the keto-mixture was analyzed by NMR (Figs. 6*B* and 8*A*). Although no intact UDP-sugar could be detected because of degradation, the structure of the putative keto-sugar could be resolved by analyzing the degradation products. From a series of one-dimensional TOCSY experiments on all of the anomeric peaks identified by a HSQC spectra, a resonance at 5.24 ppm could be identified as belonging to an expected keto-sugar. A small $J_{2,3}$ value of 3.5 Hz indicated that H-2 and H-3 are gauche to each other. The strong NOE between H-1 and H-5 indicated that H-1 and H-5 were both axial (Fig. 8*C*). The lack of NOE between H-3 and H-5 and between H-3 and H-1 indicated that H-3 is equatorial (Fig. 8, *C* and *D*). From the HSQC

spectrum the protonated carbons were assigned. From the HMBC spectrum, the quaternary carbon at C-4 and the NAc-C=O resonances were assigned. The NMR data are given in Table V. The presence of this degradation product in this mixture is consistent with the second intermediate being UDP-2-acetamido-2,6-dideoxy-β-L-*arabino*-4-hexulose. The expected UDP-2-acetamido-2,6-dideoxy-β-L-*lyxo*-4-hexulose could not be detected, either because of instability or because of an equilibrium highly in favor of the two compounds described above.

WbjC/Cap5F Reduces One of the 4-Keto-intermediates to Yield a Nucleotide-activated 2-Acetamido-2,6-dideoxy Sugar—When UDP-D-GlcNAc was incubated with WbjB and WbjC in the presence of $NADP^+$ and NADPH, the two peaks produced in the WbjB reaction decreased, and a new peak appeared in the chromatogram comigrating with the precursor sugar UDP-D-GlcNAc (Fig. 2*C*). These reaction steps could also be performed consecutively, first allowing conversion to the two 4-keto-intermediate and subsequently adding WbjC and NADPH (Fig. 9*C*). NADPH and NADH could be used equally well as hydride donors in the reduction reaction (Fig. 2, *C* and *E*).

The reduction reaction was further investigated by CE-MS analysis, which in the negative mode showed a decrease of *m/z* 606 (hydrated 2-acetamido-4-keto-2,6-dideoxy-sugar), the disappearance of *m/z* 588 (2-acetamido-4-keto-2,6-dideoxy-sugar), and the appearance of a new ion at *m/z* 590 (Fig. 3*C*). This is consistent with a reduction reaction. Additional evidence was obtained by CE-MS/MS at *m/z* 592 in the positive mode, resulting in the expected fragmentation pattern (Fig. 4*D*). Again, CE as well as CE-MS experiments using the *Staphylococcus* protein Cap5F gave identical results (data not shown).

Finally, the reduction product was purified by anion exchange chromatography and analyzed by NMR spectroscopy (Figs. 6*C* and 10*A*). From one-dimensional TOCSY experiments, the small coupling constants for protons within the ring indicated a talose configuration. The observed coupling constants for $J_{1,2}$ = 1.5 Hz, $J_{2,3}$ = 3.2 Hz, $J_{3,4}$ = 3.6 Hz, and $J_{4,5} \approx 1$ Hz were similar to their respective *J* values of 1.5, 3.0, 3.0, and 1.0 Hz observed for synthetic talose oligosaccharides (43). The strong NOE between H-1 and H-3, between H-1 and H-5, and between H-3 and H-5 indicated that H-1, H-3, and H-5 were axial (Fig. 10, *C* and *D*). From the HSQC spectrum, the protonated carbons were assigned. From the HMBC spectrum, the NAc-C=O resonances were assigned. The NMR data are

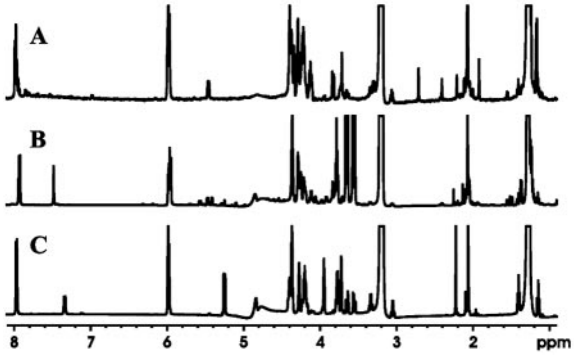

FIG. 6. **^{1}H spectra of intermediates in UDP-L-FucNAc biosynthesis.** *A*, sample containing UDP-2-acetamido-2,6-dideoxy-α-D-*xylo*-4-hexulose. *B*, sample containing degradation products from a mixture of UDP-2-acetamido-2,6-dideoxy-α-D-*xylo*-4-hexulose and UDP-2-acetamido-2,6-dideoxy-β-L-*arabino*-4-hexulose. *C*, sample containing UDP-2-acetamido-2,6-dideoxy-β-L-talose. Varying amounts of UMP were also present in each sample. Peaks from the triethylammonium salt (1.3 and 3.2 ppm) and glycerol (3.6, 3.7, and 4.1 ppm) could also observed.

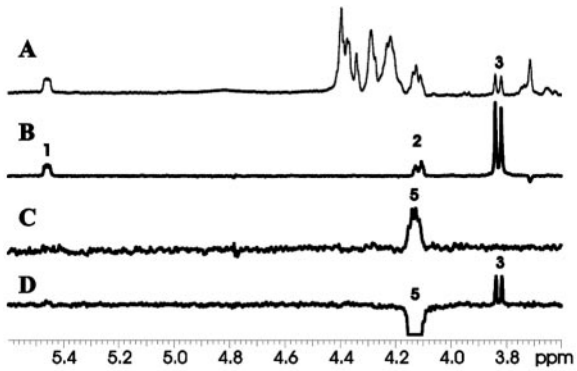

FIG. 7. **NMR analysis of UDP-2-acetamido-2,6-dideoxy-α-D-*xylo*-4-hexulose.** *A*, ^{1}H spectrum. *B*, one-dimensional TOCSY (H-3). *C*, one-dimensional TOCSY (H-6). *D*, one-dimensional TOCSY-NOESY (H-6 and H-5).

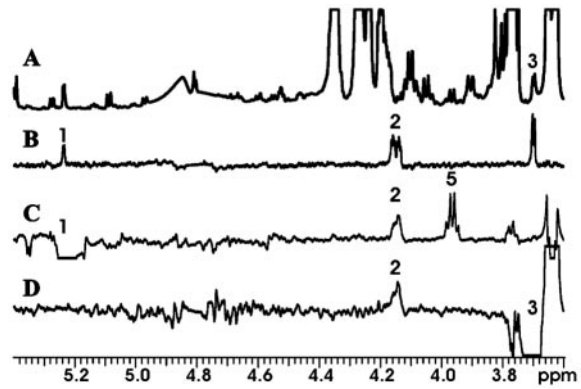

FIG. 8. **NMR analysis of UDP-2-acetamido-2,6-dideoxy-β-L-*arabino*-4-hexulose.** *A*, ^{1}H spectrum of a sample containing degradation products from a mixture of UDP-2-acetamido-2,6-dideoxy-α-D-*xylo*-4-hexulose and UDP-2-acetamido-2,6-dideoxy-β-L-*arabino*-4-hexulose. *B*, one-dimensional TOCSY (NH). *C*, one-dimensional NOESY (H-1). *D*, one-dimensional NOESY (H-3).

TABLE V
NMR analysis of intermediate compounds during UDP-L-FucNAc biosynthesis

Compound		^{1}H and ^{13}C chemical shifts, δ (ppm), and proton coupling constants, $J_{H,H}$								
		H-1 C-1 J(1,2)	H-2 C-2 J(2,3)	H-3 C-3 J(3,4)	H-4 C-4 J(4,5)	H-5 C-5 J(5,6)	H-6 C-6	NH J(H,NH)	NAc-CH3	NAc-CO
						Hz				
xylo-Sugar	δ_H	5.45	4.11	3.82		4.13	1.25		2.07	
	δ_C	94.5	52.8	71.8	93.4	70.1	11.6		22.2	175.2
	$J_{H,H}$	3.6	10.8			6.6				
arabino-Sugar	δ_H	5.24	4.15	3.7		3.96	1.23	7.43	2.05	
	δ_C	92.1	53.9	72.7	93.8	73.1	12.3		22.9	175.8
	$J_{H,H}$	2.2	3.5			6.5		9.5		
6-Deoxy-TalNAc	δ_H	5.25	4.4	3.95	3.72	3.77	1.29	7.34	2.06	
	δ_C	95.7	53.3	68.5	70.8	73.2	16.3		23.5	175.1
	$J_{H,H}$	1.5	4.3	3.6	<1	6.3		10.3		

given in Table V. Taken together, the reduction product generated by WbjC is UDP-2-acetamido-2,6-dideoxy-β-L-talose.

WbjD/Cap5G Is a Putative C-2-Epimerase Catalyzing the Formation of UDP-L-FucNAc—As described above, WbjD shows moderate homologies to UDP-D-GlcNAc 2-epimerases. Indeed, this enzyme appears to catalyze an equilibrium reaction, as would be expected of an epimerase. The peak corresponding to the 2-acetamido-2,6-dideoxy sugar synthesized in the first three reaction steps decreased significantly, and a new peak migrating slightly faster appeared (Fig. 2, *D* and *F*). Approximately 45% of the reduction product was converted to this new peak. Again, this final product could be observed either when all enzymes and cofactors were added simultaneously at the beginning of the reaction or when the reaction steps were carried out consecutively (Fig. 9*D*).

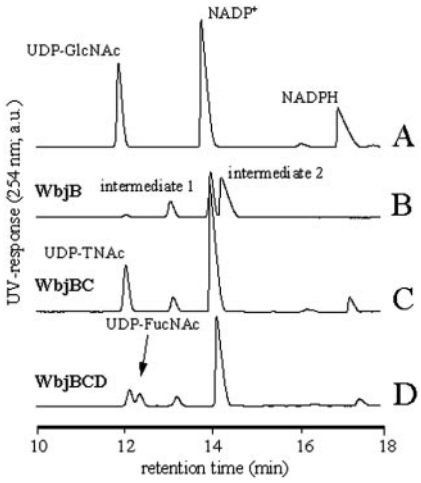

FIG. 9. **CE analysis of UDP-L-FucNAc biosynthesis.** *A*, standard, UDP-D-GlcNAc, $NADP^+$ and NADPH. *B*, UDP-D-GlcNAc, converted with WbjB and $NADP^+$ (*intermediates 1* and *2* represent the two 2,6-dideoxy-2-amino-4-keto-hexose intermediates). *C*, UDP-D-GlcNAc, converted with WbjB and $NADP^+$, followed by WbjC and NADPH (UDP-TNAc refers to UDP-2-acetamido-2,6-dideoxy-L-talose). *D*, UDP-D-GlcNAc, converted with WbjB and $NADP^+$, followed by WbjC and NADPH, and followed by WbjD. *a.u.*, arbitrary units.

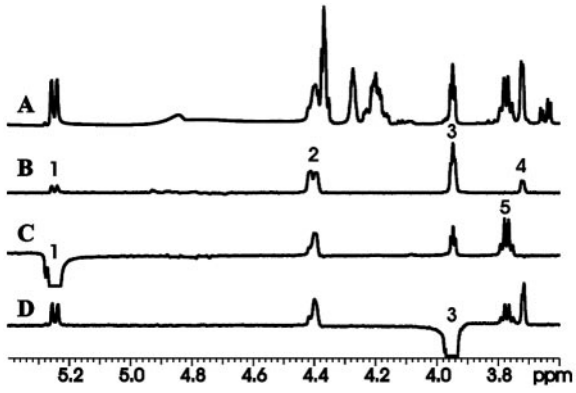

FIG. 10. **NMR analysis of UDP-2-acetamido-2,6-dideoxy-β-L-talose.** *A*, ^1H spectrum. *B*, one-dimensional TOCSY (NH). *C*, one-dimensional NOESY (H-1). *D*, one-dimensional NOESY (H-3).

CE-MS analysis was carried out to investigate this new product. As expected from an epimerization reaction, no changes could be observed compared with the mass spectra obtained from the WbjC-catalyzed reaction (Fig. 3*D*). The fragmentation pattern in CE-MS/MS analysis at *m/z* 592 (positive mode) looked exactly the same as before the epimerization step (Fig. 4*D*; *m/z* 592 spectra only shown once). This is consistent with the formation of the 2-epimer of UDP-TalNAc, *i.e.* UDP-L-Fuc2NAc. The *Staphylococcus* homolog Cap5G yielded the same results, except for inactivity of the enzyme at 37 °C. The Cap5G reaction had to be performed at 30 °C (data not shown).

Three Enzymes Catalyze a Five-step Reaction Cascade Converting UDP-D-GlcNAc to a Product Consistent with UDP-L-FucNAc—We propose the following reaction scheme for the biosynthesis pathway of nucleotide-activated L-FucNAc (Fig. 11). WbjB/Cap5E catalyzes 4,6-dehydration, 5-epimerization, and 3-epimerization of the precursor UDP-D-GlcNAc, resulting in as many as three intermediates, namely UDP-2-acetamido-2,6-dideoxy-D-*xylo*-4-hexulose, UDP-2-acetamido-2,6-dideoxy-L-*arabino*-4-hexulose, and UDP-2-acetamido-2,6-dideoxy-L-*lyxo*-4-hexulose, which are present in the ketal form. The next step is reduction at C-4 to yield UDP-2-acetamido-2,6-dideoxy-L-talose, catalyzed by WbjC/Cap5F. Finally, the UDP-2-acetamido-2,6-dideoxy-L-talose 2-epimerase WbjD/Cap5G partially converted UDP-2-acetamido-2,6-dideoxy-L-talose to a product that is consistent with UDP-L-FucNAc in a C-2-epimerization reaction.

Inactivation of wbjB Abrogates B-band O Antigen Production in P. aeruginosa PA103—A nonpolar gene knockout of *wbjB* has been constructed by insertional mutation with a gentamicin resistance cassette and allelic replacement. Strain BK103B with *wbjB*::*aacC1* on its chromosome no longer produces B-band O antigen. In the silver-stained LPS-SDS-PAGE gel, only the banding pattern of A-band O antigen is visible (Fig. 12*A*). The presence of A-band O antigen was confirmed by Western immunoblotting analysis using the mAb N1F10 (Fig. 12*D*). Moreover, LPS of the mutant does not react with polyclonal or mAbs to O11 B-band (Fig. 12, *B* and *C*). It has to be noted that mAb MF55-1 reacts with low molecular weight O11 B-band. Production of the serospecific O antigen in the mutant strain BK103B could be restored by adding *P. aeruginosa wbjB* or the *S. aureus* gene *cap5E* on an *E. coli*/P. aeruginosa shuttle vector (Fig. 12, *A–C*).

Knockout of cap5E or cap5F and cap5G Results in Nonencapsulated S. aureus Mutants—*S. aureus* strain NCTC 8325

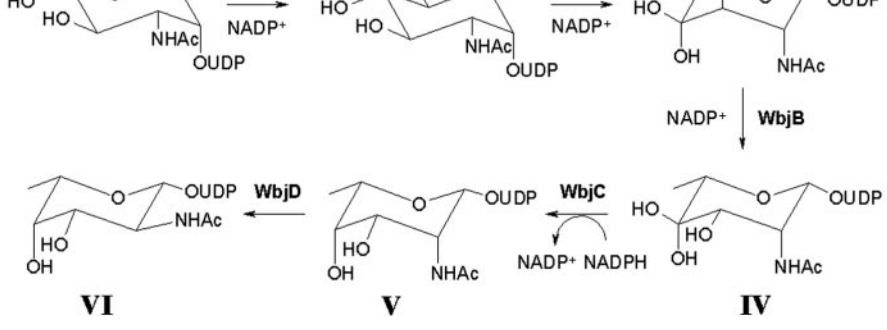

FIG. 11. **Proposed biosynthesis pathways leading to UDP-L-FucNAc.** *I*, UDP-α-D-GlcNAc. *II*, UDP-2-acetamido-2,6-dideoxy-α-D-*xylo*-4-hexulose. *III*, UDP-2-acetamido-2,6-dideoxy-β-L-*arabino*-4-hexulose, *IV*, UDP-2-acetamido-2,6-dideoxy-β-L-*lyxo*-4-hexulose. *V*, UDP-2-acetamido-2,6-dideoxy-β-L-talose. *VI*, UDP-β-L-FucNAc.

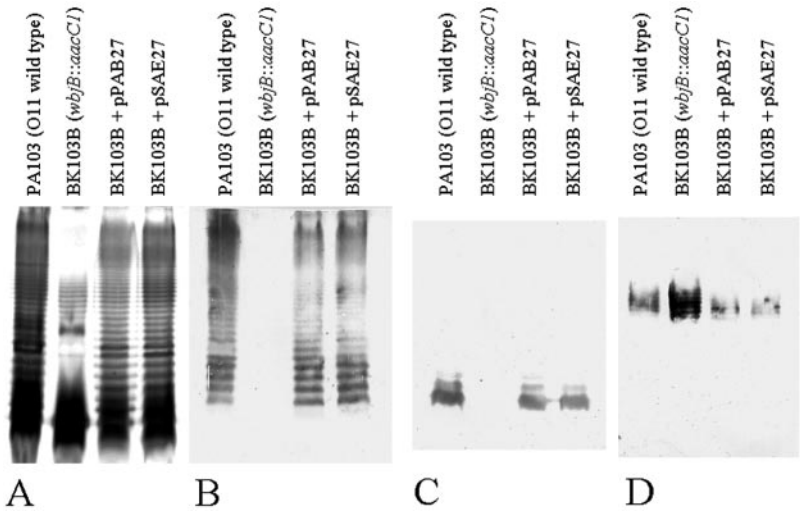

FIG. 12. **Knockout and complementation analysis of *wbjB*.** *A*, silver-stained LPS-SDS-PAGE gel. *B*, Western immunoblotting analysis with polyclonal antiserum to B-band O antigen of serotype O11. *C*, Western immunoblotting analysis with mAb MF55-1 (specific against B-band O antigen of serotype O11). *D*, Western immunoblotting analysis with mAb N1F10 (specific for A-band O antigen).

carries a complete *cap5* locus but fails to produce CP5. Genomic analysis of the *cap5E* gene from this strain (sequence of 8325 available at www.genome.ou.edu/staph.html) revealed that it carried a single amino acid mutation (Met^{134} to Arg^{134}) within Cap5E. Wann and colleagues (44) demonstrated that *cap5E* provided *in trans* restored CP5 expression to NCTC 8325-4. We insertionally inactivated the *cap5F* gene by deleting 126 bp of the gene and replacing it with an *ermB* cassette. Allelic replacement of the native gene with this disrupted copy resulted in a CP-negative phenotype. Complementation of this mutation was observed when a plasmid containing the *cap5* promoter region and genes *cap5A* through *cap5F* was introduced into mutant F4. No complementation was observed with the same plasmid containing only the *cap* genes *5A* through *5E*. Mutagenesis of *cap5G* in strain Newman was achieved by deleting a 294-bp region of the gene and replacing it with an *ermB* cassette. The resultant strain GO1 displayed a CP-negative phenotype that could be restored by *cap5G* cloned in the vector pLI50. Fig. 13 shows a colony immunoblot of *cap5E*, *cap5F*, and *cap5G* mutants that failed to produce CP and the complemented strains with the restoration of CP production.

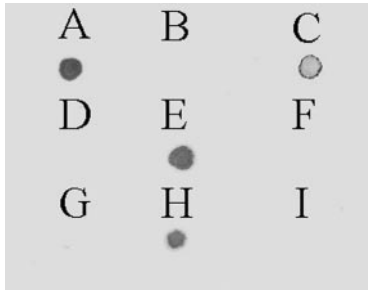

FIG. 13. **Knockout and complementation analysis of *S. aureus* *cap5E*, *cap5F*, and *cap5G*.** Colony immunoblot analysis with polyclonal antiserum to CP5. *A*, Newman $CP5^+$. *B*, 8325-4 $CP5^-$ (mutation in *cap5E*). *C*, 8325-4 (pCAP16). *D*, strain G01 (*ermB* in *cap5G*). *E*, GO1 (pKOR2). *F*, G01 (pLI50). *G*, strain F4 (*ermB* in *cap5F*). *H*, F4 (pCAP17). *I*, F4 (pCAP16).

DISCUSSION

This report describes for the first time the biosynthesis steps from the precursor UDP-D-GlcNAc to a nucleotide precursor sugar that is consistent with UDP-L-FucNAc; five distinct enzymatic steps, catalyzed by three enzymes, are sufficient. The deduced amino acid sequences of the gene products from *P. aeruginosa* and *S. aureus* are highly homologous. WbjB and Cap5E show 67% identity and 81% similarity over 332 amino acids. Similarly, WbjC and Cap5F share 40% identity and 59% similarity over 370 amino acids. The last enzymes in the pathway, WbjD and Cap5G, were also highly homologous, with 57% identity and 71% similarity over 377 amino acids.

Two putative pathways for the biosynthesis of UDP-L-FucNAc have been proposed in the literature, both involving UDP-D-ManNAc as the precursor (15, 20). Hypothesizing putative pathways based solely on *in silico* analysis is prone to error, because occasionally the primary protein sequences of enzymes are highly homologous even though they catalyze completely different conversions. This is especially true for SDR proteins, which include dehydratases, dehydrogenases, epimerases, isomerases, and reductases. Members of this family play crucial roles in the biosynthesis of nucleotide-activated sugars throughout prokaryotes and eukaryotes, in steroid biosynthesis, and in alcohol metabolism (40). Typically, they have the nucleotide-binding motif G*XXG*X*XG* or G*XXXG*X*G* near the N terminus that is essential for coenzyme binding (41). Moreover, they all share a motif Y*XXX*K, the active site. This motif can be extended to the so-called catalytic triad SYK. Recently, SMK has been described as a slight modification of this triad in WbpM from *P. aeruginosa*, an enzyme that is putatively involved in UDP-*N*-acetyl-D-fucosamine/quinovosamine biosynthesis from UDP-D-GlcNAc (42). FlaA1 from *Helicobacter pylori*, catalyzing the same reaction as WbpM, has an SYK catalytic triad (45). Interestingly, of the two SDR proteins involved in UDP-L-FucNAc-biosynthesis, one has SMK (WbjB/Cap5E) and the other has SYK (WbjC/Cap5F). WbjB/Cap5E, WbjC/Cap5F, and WbpM/FlaA1 are highly homologous and yet catalyze distinct reaction steps in nucleotide-activated sugar biosynthesis. Thus, it is not surprising that UDP-L-FucNAc biosynthesis follows a pathway different from those proposed previously by Jiang *et al.* (15) and Lee and Lee, respectively (20). Limitations of the proposals have been taken into account by these research groups. The most efficient way to analyze biochemical pathways is through enzymatic assays. For the third enzyme involved in UDP-L-FucNAc biosynthesis, it was easier to propose a putative function based solely on its significant homologies to UDP-D-GlcNAc 2-epimerases, which do not belong to the diverse SDR protein family.

Our results showed that WbjB/Cap5E has at least two functions with both 4,6-dehydratase and 5-epimerase activities. Most likely, it also catalyzes epimerization at C-3. Bifunctionality within the SDR protein family also was reported for Gmd from *Aneurinibacillus thermoaerophilus*, which has been described as 4,6-dehydratase/4-reductase converting GDP-D-mannose to GDP-D-rhamnose (46), and for hFX, a 3,5-epime-

rase/4-reductase involved in the biosynthesis of GDP-L-fucose (47). The first reaction step catalyzed by WbjB/Cap5E is 4,6-dehydration, which appears to be quantitative, because CE analysis revealed no UDP-D-GlcNAc left on conversion. The second reaction step of WbjB/Cap5E is an equilibrium reaction, as would be expected for an epimerase reaction.

Using CE, coupled CE-MS, and NMR analyses, we were able to show the reaction cascade that converts UDP-D-GlcNAc into a product that is consistent with UDP-L-FucNAc. CE analysis of the WbjB/Cap5E-catalyzed reaction showed a quantitative conversion of UDP-D-GlcNAc to two new nucleotide-activated sugars. To investigate these two peaks further, coupled CE-MS was performed. Surprisingly, MS showed a mixture of two peaks with *m/z* ratios of 588 and 606. A 4,6-dehydration is supposed to result in loss of water and thus a peak at *m/z* 588 only. Two peaks could correspond to a bifunctional enzyme with both 4,6-dehydratase and 3,5-epimerase activity. Time course experiments with CE-MS/MS/MS clearly demonstrated that the peak at *m/z* 606 is not UDP-D-GlcNAc. Loss of a fragment ion of *m/z* 138 indicated the removal of the hydroxyl group at C-6, because a −30 shift (generation of formaldehyde) is characteristic of hexoses. Thus, water has been added to the hexose moiety after 4,6-dehydration. There are two possibilities for this scenario: formation of a geminal diol at the keto-group at C-4 or ring opening to result a nucleotide-activated sugar in the open form. Because the final assignments could not be accomplished using an MS approach, we decided to purify the two putative keto-intermediates for NMR analysis, despite their expected instability (46, 48, 49). The purification of the intermediate compound, which migrated faster than $NADP^+$ during CE analysis, was achieved by anion exchange chromatography. The compound proved to be unstable, partially decomposing to the monosaccharide and UDP, but its structure could be elucidated using nanoprobe NMR. One-dimensional TOCSY and one-dimensional TOCSY-NOESY allowed assignment of the hydrogens on C-1, C-2, C-3, C-5, and C-6, as well as on the acetyl group. Lack of a hydrogen at C-4 and lack of a second ^{13}C signal in the keto-range indicated the presence of a ketal at C-4, thus excluding the possibility of an open sugar. The quaternary carbon could be assigned by HMBC. The other carbons were assigned with HSQC. Thus, the structure of this intermediate sugar is UDP-2-acetamido-2,6-dideoxy-α-D-*xylo*-4-hexulose, resulting from 4,6-dehydration of UDP-D-GlcNAc. Anion exchange chromatography did not yield a second compound. Therefore, we concentrated a WbjB reaction mix and, after addition of D_2O, analyzed this mixture by NMR spectroscopy. Using similar selective techniques as with the other intermediate compound, we were able to assign a second structure, UDP-2-acetamido-2,6-dideoxy-β-L-*arabino*-4-hexulose, which is formed by 5-epimerization of UDP-2-acetamido-2,6-dideoxy-α-D-*xylo*-4-hexulose. These data suggested that WbjB/Cap5E most likely has 4,6-dehydratase, 5-epimerase, and 3-epimerase activities. The lack of the expected final product of this reaction cascade, namely UDP-2-acetamido-2,6-dideoxy-β-L-*lyxo*-4-hexulose, may be due to the highly unstable *lyxo*-product or an equilibrium favoring the first two intermediates, UDP-2-acetamido-2,6-dideoxy-α-D-*xylo*-4-hexulose and UDP-2-acetamido-2,6-dideoxy-β-L-*arabino*-4-hexulose. An alternative possibility would be a bifunctional enzyme WbjC/Cap5F with both 3-epimerase/4-reductase activities. However, because we are not able to purify either UDP-2-acetamido-2,6-dideoxy-β-L-*arabino*-4-hexulose or UDP-2-acetamido-2,6-dideoxy-β-L-*lyxo*-4-hexulose, we are not able to investigate this scenario further.

The next reaction step in the biosynthesis of UDP-L-FucNAc involves the conversion of the intermediate sugars into a new compound that comigrated with the precursor UDP-D-GlcNAc in CE analysis. NADH as well as NADPH could be used as hydride donor. CE-MS analysis showed a new peak at *m/z* 590, which would be expected after reduction of the keto-intermediate. CE-MS/MS experiments provided further evidence that the reduction was on the hexose moiety of the nucleotide-activated sugars. To complete identification of this compound, we purified the reduction product using anion exchange chromatography. The sugar was concentrated and, after addition of D_2O, was analyzed by NMR. Unlike the unstable keto-intermediates, this sugar turned out to be highly stable. One-dimensional TOCSY, one-dimensional NOESY, and other techniques demonstrated that the WbjC/Cap5F reduction product is UDP-2-acetamido-2,6-dideoxy-β-L-talose, sometimes referred to as UDP-L-pneumosamine or UDP-L-*N*-acetylpneumosamine (PneNAc) (50). Interestingly, the CP of *S. pneumoniae* type 5 is composed not only of D-glucose and D-glucuronic acid but also of 2-acetamido-2,6-dideoxy-D-*xylo*-4-hexulose, L-PneNAc, and L-FucNAc (50). Thus, three of the intermediates and final products of the pathway described in the present study are part of the type 5 capsular polysaccharide. Unfortunately, no nucleotide sequence data of *S. pneumoniae* type 5 biosynthesis locus are yet available. Based on the biochemical characterization of the Wbj and Cap proteins, one can predict that homologs of WbjB/Cap5E, WbjC/Cap5F, and WbjD/Cap5G will be present in the corresponding *S. pneumoniae* type 5 gene cluster.

The last step of the UDP-L-FucNAc biosynthesis pathway would require C-2-epimerization of UDP-2-acetamido-2,6-dideoxy-β-L-talose. WbjD/Cap5G is moderately homologous to the *S. aureus* UDP-D-GlcNAc 2-epimerase (Cap5P). As expected, WbjD/Cap5G catalyzed UDP-2-acetamido-2,6-dideoxy-β-L-talose to produce a new sugar peak, as detected by CE analysis. Further experiments have been performed using CE-MS. The fragmentation pattern did not change on this reaction from the one obtained for UDP-2-acetamido-2,6-dideoxy-β-L-talose, which is consistent with epimerization. As mentioned above, UDP-2-acetamido-2,6-dideoxy-β-L-talose proved to be a very stable sugar, unlike the final reaction product. When purified UDP-2-acetamido-2,6-dideoxy-β-L-talose was incubated with WbjD, UDP was produced by decomposition of the final product UDP-L-FucNAc to the monosaccharide and the nucleotide as observed by CE. Based on this experience and the following reasons, we were not able to pursue NMR analysis of UDP-L-FucNAc, the putative product of the WbjD reaction. First, the unstable nature of this sugar nucleotide posed difficulty in its preparation. Second, the epimerization activity of WbjD yielded a mixture of UDP-TalNAc and UDP-Fuc2NAc. Our CE (Fig. 2*F*) and CE-MS-MS results (Fig. 3*D*) support these findings. The proportion of UDP-Fuc2NAc was small in the mixture, thus making it difficult to purify and resolve the two compounds. Another piece of evidence to support our interpretation that WbjD and its homolog Cap5G in *S. aureus* are C2-epimerases is the fact that L-FucNAc is a common sugar residue shared by the O-polysaccharide of *P. aeruginosa* O11 and the type 5 capsular polysaccharide of *S. aureus*. Therefore, once we were able to prove that UDP-TalNAc is formed by the activity of WbjC/Cap5F, we clearly correlated the activities of the first two enzymes to the modification of C-3, C-4, C-5, and C-6 of the substrate, UDP-GlcNAc. The only logical reaction to follow is C-2-epimerization to produce UDP-Fuc2NAc, and our data obtained from CE and CE-MS-MS support this interpretation.

It was intriguing to observe that UDP-L-FucNAc acted as an inhibitor of WbjB/Cap5E. When all of the enzymes were added simultaneously, more NADPH was left in the reaction mixture than when the enzymes were added sequentially, allowing each

step to go to completion. CE-MS clearly demonstrated that some UDP-D-GlcNAc was still left after the simultaneous reaction. No UDP-D-GlcNAc could be detected when the reactions were done consecutively. Feedback inhibition is a common way to regulate nucleotide-activated sugar biosynthesis, as in GDP-L-fucose biosynthesis, in which the final product, GDP-β-L-fucose, acts as an inhibitor of Gmd (51).

The cofactor dependence of WbjB/Cap5E proved to be crucial. The absence of any added cofactor or the addition of NAD^+ instead of $NADP^+$ resulted in almost no conversion at all. The conversion observed (<5%) was most likely due to $NADP^+$ bound to the enzyme even during protein purification. In contrast, WbjC/Cap5F used both NADH and NADPH as hydride donors in the reduction reaction. Because of the lack of commercially available substrate, kinetic parameters have not been investigated. 4-Keto-sugars have frequently been described in the literature as unstable (46, 48, 49). Our report confirms these studies, because the keto-intermediates involved in this pathway readily decompose to the corresponding monosaccharides and UDP. Because the first enzyme acting in the pathway is multifunctional, a coupled assay using both WbjB/Cap5E and WbjC/Cap5F would not result in proper kinetic data of the WbjC/Cap5F-catalyzed reduction reaction. However, such coupling could be a convenient means to at least qualitatively screen for inhibitors of WbjB/Cap5E and WbjC/Cap5F by measuring the decrease of NADH or NADPH using $A_{340\,nm}$. The use of both hydride donors has also been described for Gmd and Rmd in GDP-D-rhamnose biosynthesis (46) as well as for RmlD in dTDP-L-rhamnose biosynthesis (48).

The construction of a knockout mutant of the first gene (*wbjB*) involved in the biosynthesis of UDP-L-FucNAc clearly demonstrated that the corresponding enzyme WbjB is unmistakably involved in the biosynthesis of B-band O antigen in *P. aeruginosa* serotype O11. Inactivation of *wbjB* resulted in complete loss of B-band O antigen, as detected by silver staining of an SDS-PAGE resolved LPS and by Western immunoblotting analysis with polyclonal or monoclonal antibodies to serotype O11 (Fig. 12, *A–C*). The banding pattern of LPS isolated from the mutant BK103B was due to A-band O antigen, as was proven by the use of mAb N1F10 specific for A-band O antigen (Fig. 12, *A* and *D*). The *P. aeruginosa* gene *wbjB* and its *S. aureus* homolog *cap5E* were able to restore production of B-band O antigen fully, when provided on an *E. coli*/P. aeruginosa shuttle vector pUCP27. The three *cap5* genes *cap5E*, *cap5F*, and *cap5G* are all required for capsule synthesis in *S. aureus*. In this study, the insertional inactivation of *cap5F* and *cap5G* confirmed the essential role of these genes in CP5 production. A previous study had identified that a naturally occurring mutation in strain 8325-4 could be mapped to *cap5E* (39). However, it is apparent only from analysis of the recently available genomic sequence that this mutation arose from a single amino acid change (Met^{134} to Arg^{134}) in the SMK domain, underlining the important catalytic role of this triad. The data described here represent a "proof of principle" that the genes coding for the enzymes catalyzing the biosynthesis of UDP-L-FucNAc are conserved among Gram-positive and Gram-negative bacteria and can functionally cross-complement each other fully.

In conclusion, we propose a novel biosynthetic pathway for UDP-L-FucNAc, which is the putative precursor of L-FucNAc in both Gram-positive and Gram-negative bacteria. The data in this study suggest the respective function of the three proteins to be: (i) WbjB/Cap5E is a trifunctional UDP-D-GlcNAc 4,6-dehydratase/5-epimerase/3-epimerase, (ii) WbjC/Cap5F is a UDP-2-acetamido-2,6-dideoxy-β-L-*lyxo*-4-hexulose 4-reductase, and (iii) WbjD/Cap5G is likely a UDP-2-acetamido-2,6-dideoxy-β-L-talose 2-epimerase. The enzymes involved are promising targets in the search for new broad spectrum antibiotics. Work is under way to develop assays suitable to screen compound libraries for potential inhibitors.

Acknowledgments—We appreciate the excellent technical assistance of Martha Fordinal and the helpful microbiological input of Mauricia Matewish. Nicolas Cadotte and Suzon Larocque are gratefully acknowledged for performing the NMR experiments. We thank Anthony W. Chow (University of British Columbia, Vancouver, Canada) for providing *S. aureus* serotype 5. Timothy Foster (Trinity College, Dublin) generously provided pCAP16 and pCAP17, and Kevin Kiser constructed pERMB and pKBK6a. We acknowledge Lingyi Deng for helpful discussions. The authors are also thankful to the Canadian Bacterial Diseases Network, a consortium of the Federal Networks of Centers of Excellence program, for providing a small travel grant to allow B. K. to perform CE/MS experiments at the Institute for Biological Sciences, National Research Council of Canada in Ottawa.

REFERENCES

1. Raetz, C. R. (1990) *Annu. Rev. Biochem.* **59,** 129–170
2. Rocchetta, H. L., Burrows, L. L., and Lam, J. S. (1999) *Microbiol. Mol. Biol. Rev.* **63,** 523–553
3. Liu, P. V., Matsumoto, H., Kusama, H., and Bergan, T. (1983) *Int. J. Sys. Bacteriol.* **33,** 256–264
4. Liu, P. V., and Wang, S. (1990) *J. Clin. Microbiol.* **28,** 922–925
5. Cryz, S. J., Jr., Pitt, T. L., Furer, E., and Germanier, R. (1984) *Infect. Immun.* **44,** 508–513
6. Lowy, F. D. (1998) *N. Engl. J. Med.* **339,** 520–532
7. Thakker, M., Park, J. S., Carey, V., and Lee, J. C. (1998) *Infect. Immun.* **66,** 5183–5189
8. Portoles, M., Kiser, K. B., Bhasin, N., Chan, K. H., and Lee, J. C. (2001) *Infect. Immun.* **69,** 917–923
9. Knirel, Y. A., and Kochetkov, N. K. (1994) *Biochemistry* (*Moscow*) **59,** 1325–1383
10. Moreau, M., Richards, J. C., Fournier, J. M., Byrd, R. A., Karakawa, W. W., and Vann, W. F. (1990) *Carbohydr. Res.* **201,** 285–297
11. Fournier, J. M., Vann, W. F., and Karakawa, W. W. (1984) *Infect. Immun.* **45,** 87–93
12. Jones, C., Currie, F., and Forster, M. J. (1991) *Carbohydr. Res.* **221,** 95–121
13. Manca, M. C., Weintraub, A., and Widmalm, G. (1996) *Carbohydr. Res.* **281,** 155–160
14. Kasper, D. L., Weintraub, A., Lindberg, A. A., and Lonngren, J. (1983) *J. Bacteriol.* **153,** 991–997
15. Jiang, S. M., Wang, L., and Reeves, P. R. (2001) *Infect. Immun.* **69,** 1244–1255
16. Pitt, T. L. (1988) *Eur. J. Clin. Microbiol. Infect. Dis.* **7,** 238–247
17. Pavlovskis, O. R., Pollack, M., Callahan, L. T., III, and Iglewski, B. H. (1977) *Infect. Immun.* **18,** 596–602
18. Sompolinsky, D., Samra, Z., Karakawa, W. W., Vann, W. F., Schneerson, R., and Malik, Z. (1985) *J. Clin. Microbiol.* **22,** 828–834
19. Alpern, E. R., Alessandrini, E. A., McGowan, K. L., Bell, L. M., and Shaw, K. N. (2001) *Pediatrics* **108,** E23
20. Lee, J. C., and Lee, C. Y. (1999) in *Genetics of Bacterial Polysaccharides* (Goldberg, J. B., ed) pp. 185–205, CRC Press, Boca Raton, FL
21. Yanisch-Perron, C., Vieira, J., and Messing, J. (1985) *Gene* (*Amst.*) **33,** 103–119
22. Simon, R., Priefer, U., and Puhler, A. (1983) *BioTechnology* **1,** 784–791
23. Laemmli, U. K. (1970) *Nature* **227,** 680–685
24. Bradford, M. M. (1976) *Anal. Biochem.* **72,** 248–254
25. Hitchcock, P. J., and Brown, T. M. (1983) *J. Bacteriol.* **154,** 269–277
26. Fomsgaard, A., Freudenberg, M. A., and Galanos, C. (1990) *J. Clin. Microbiol.* **28,** 2627–2631
27. Lam, J. S., MacDonald, L. A., Lam, M. Y., Duchesne, L. G., and Southam, G. G. (1987) *Infect. Immun.* **55,** 1051–1057
28. Lam, M. Y., McGroarty, E. J., Kropinski, A. M., MacDonald, L. A., Pedersen, S. S., Hoiby, N., and Lam, J. S. (1989) *J. Clin. Microbiol.* **27,** 962–967
29. Lee, J. C., Liu, M. J., Parsonnet, J., and Arbeit, R. D. (1990) *J. Clin. Microbiol.* **28,** 2612–2615
30. Altschul, S. F., Madden, T. L., Schaffer, A. A., Zhang, J., Zhang, Z., Miller, W., and Lipman, D. J. (1997) *Nucleic Acids Res.* **25,** 3389–3402
31. Corpet, F. (1988) *Nucleic Acids Res.* **16,** 10881–10890
32. Sambrook, J., Fritsch, E. F., and Maniatis, T. (1989) *Molecular Cloning: A Laboratory Manual*, Cold Spring Harbor Laboratory, Cold Spring Harbor, NY
33. Newton, D. T., and Mangroo, D. (1999) *Biochem. J.* **339,** 63–69
34. Koplin, R., Brisson, J. R., and Whitfield, C. (1997) *J. Biol. Chem.* **272,** 4121–4128
35. Brisson, J. R., Sue, S. C., Wu, W. G., McManus, G., Nghia, P. T., and Uhrin, D. (2002) in *NMR Spectroscopy of Glycoconjugates* (Jimenez-Barbero, J., and Peters, T., eds) pp. 59–93, Wiley-VCH, Weinhem, Germany
36. Schweizer, H. P., and Hoang, T. T. (1995) *Gene* (*Amst.*) **158,** 15–22
37. Lee, J. C. (1995) *Methods Mol. Biol.* **47,** 209–216
38. Kasatiya, S. S., and Baldwin, J. N. (1967) *Can. J. Microbiol.* **13,** 1079–1086
39. Kiser, K. B., Bhasin, N., Deng, L., and Lee, J. C. (1999) *J. Bacteriol.* **181,** 4818–4824
40. Jornvall, H., Hoog, J. O., and Persson, B. (1999) *FEBS Lett.* **445,** 261–264
41. Wierenga, R. K., Maeyer, M. C. H., and Hol, W. G. J. (1985) *Biochemistry* **24,** 1346–1357
42. Creuzenet, C., and Lam, J. S. (2001) *Mol. Microbiol.* **41,** 1295–1310
43. Lowary, T. L., Eichler, E., and Bundle, D. R. (2002) *Can. J. Chem.* **80,** 1112–1130

44. Wann, E. R., Dassy, B., Fournier, J. M., and Foster, T. J. (1999) *FEMS Microbiol. Lett.* **170,** 97–103
45. Creuzenet, C., Schur, M. J., Li, J., Wakarchuk, W. W., and Lam, J. S. (2000) *J. Biol. Chem.* **275,** 34873–34880
46. Kneidinger, B., Graninger, M., Adam, G., Puchberger, M., Kosma, P., Zayni, S., and Messner, P. (2001) *J. Biol. Chem.* **276,** 5577–5583
47. Sullivan, F. X., Kumar, R., Kriz, R., Stahl, M., Xu, G. Y., Rouse, J., Chang, X. J., Boodhoo, A., Potvin, B., and Cumming, D. A. (1998) *J. Biol. Chem.* **273,** 8193–8202
48. Graninger, M., Nidetzky, B., Heinrichs, D. E., Whitfield, C., and Messner, P. (1999) *J. Biol. Chem.* **274,** 25069–25077
49. Bulet, P., Hoflack, B., Porchet, M., and Verbert, A. (1984) *Eur. J. Biochem.* **144,** 255–259
50. Jansson, P. E., Lindberg, B., and Lindquist, U. (1985) *Carbohydr. Res.* **140,** 101–110
51. Bisso, A., Sturla, L., Zanardi, D., De Flora, A., and Tonetti, M. (1999) *FEBS Lett.* **456,** 370–374
52. Liu, P. V. (1973) *J. Infect. Dis.* **128,** 506–513
53. Peng, H. L., Novick, R. P., Kreiswirth, B., Kornblum, J., and Schlievert, P. (1988) *J. Bacteriol.* **170,** 4365–4372
54. Novick, R. (1967) *Virology* **33,** 155–166
55. Schweizer, H. D. (1993) *BioTechniques* **15,** 831–834
56. West, S. E., Schweizer, H. P., Dall, C., Sample, A. K., and Runyen-Janecky, L. J. (1994) *Gene* (*Amst.*) **148,** 81–86
57. Bhasin, N., Albus, A., Michon, F., Livolsi, P. J., Park, J. S., and Lee, J. C. (1998) *Mol. Microbiol.* **27,** 9–21
58. Sau, S., Sun, J., and Lee, C. Y. (1997) *J. Bacteriol.* **179,** 1614–1621
59. Lee, C. Y., Buranen, S. L., and Ye, Z. H. (1991) *Gene* (*Amst.*) **103,** 101–105
60. Sievert, D. M., Boulton, M. L., Stoltman, G., Johnson, D., Stobierski, M. G., Downes, F. P., Somsel, P. A., Rudrik, J. T., Hafeez, W., Lundstrom, T., Flanagan, E., Johnson, R., Mitchell, J., and Chang, S. (2002) *Morbidity and Mortality Weekly Report*, Vol. 51, pp. 565–567, Centers for Disease Control, Atlanta

Three Highly Conserved Proteins Catalyze the Conversion of UDP-*N*-acetyl-d-glucosamine to Precursors for the Biosynthesis of O Antigen in *Pseudomonas aeruginosa* O11 and Capsule in *Staphylococcus aureus* Type 5: IMPLICATIONS FOR THE UDP-N-ACETYL-l-FUCOSAMINE BIOSYNTHETIC PATHWAY

Bernd Kneidinger, Katie O'Riordan, Jianjun Li, Jean-Robert Brisson, Jean C. Lee and Joseph S. Lam

J. Biol. Chem. 2003, 278:3615-3627.
doi: 10.1074/jbc.M203867200 originally published online December 2, 2002
